

# 643. Rod-shaped piezoelectric actuator with radial polarization

R. Lučinskis<sup>a</sup>, D. Mažeika<sup>b</sup>, R. Daukševičius<sup>c</sup>

Vilnius Gediminas Technical University, Saulėtekio al. 11, LT-10223 Vilnius, Lithuania

E-mail: <sup>a</sup> [raimundas.lucinskis@vgtu.lt](mailto:raimundas.lucinskis@vgtu.lt), <sup>b</sup> [dalius.mazeika@vgtu.lt](mailto:dalius.mazeika@vgtu.lt), <sup>c</sup> [rolanas.dauksevicius@vgtu.lt](mailto:rolanas.dauksevicius@vgtu.lt).

(Received 21 March 2011; accepted 15 May 2011)

**Abstract.** This paper analyzes contact point trajectories of the rod-type piezoelectric actuator, which has circular cross-section and is characterized by the non-uniform polarization. Radial polarization is used to achieve flexural oscillations in perpendicular planes and to increase number of degrees of freedom of the contact point movement. Particular electrode pattern of the actuator was determined and contact point trajectories were studied under different excitation regimes. A prototype of piezoelectric actuator was developed and experimental measurements of contact point trajectories were performed. The results of numerical modeling and experimental study are compared and discussed.

**Keywords:** piezoelectric actuator, multi-DOF, radial polarization.

## 1. Introduction

One of the current trends of technological development of the piezoelectric actuators is associated with miniaturization and reduction of design complexity [1]. The main objective of such systems development is to design a micro-scale system that has particular functionality and simple structural design. Development of the miniature actuators with multiple degrees of freedom (multi-DOF actuators) is relevant for such devices as mobile phones, personal digital assistants, cameras and etc. [1, 2].

Various design principles are used for the development of actuators but the majority of multi-DOF actuators are based on superposition of longitudinal and flexural vibrations of the structure [1, 2].

Present study reports results of investigation of a piezoelectric actuator that is characterized as a metal rod excited by piezoelectric cylinder with radial direction of polarization. Design of the actuator is based on bulk cylinder-type piezoelectric actuator with central wired electrode proposed by prof. R. Bansevicius [3, 4,7] but the developed version has some improvements. Metal rod is introduced as new design element and hollow piezoceramic cylinder is used instead of the bulk cylinder into design and is used as vibrator while hollowed piezoceramic cylinder is used for excitation and control of the vibrations. Operating principle of the actuator is based on superposition of longitudinal and flexural modes.

The performed work demonstrates that the proposed radially-polarized piezoelectric actuator is an effective solution for generation of a multi-DOF motion and. the actuator can control contact point trajectory by means of a specific topology of the electrodes and excitation regimes. The paper presents results of the numerical modeling as well as experimental obtained in the course of testing of the fabricated prototype of the actuator. The research work is finalized with formulation of the conclusions.

## 2. Design of piezoelectric actuator

Proposed piezoelectric actuator consists of a core metal rod placed inside piezoceramic hollow cylinder coated by thin silver electrode (Fig. 1). The outer diameter of the core rod is fit

to the inner diameter of the piezoceramic cylinder. Cylinder has radial polarization and polarization vector at each point of the cylinder is perpendicular to longitudinal axis and oriented in outward direction with respect to cylinder surface. The metal rod is grounded and operates as a stator. Rod is used as internal electrode of the actuator as well. The surface of the outer electrode is divided into four sections 1, 2, 3, 4 with respect to the perimeter of the cylinder and three sections a, b, c along cylinder length. The dimensions of the piezoelectric actuator are chosen so that the resonant frequency of the 1<sup>st</sup> longitudinal mode coincides with the 3<sup>rd</sup> flexural mode. The required vibration mode is achieved in a selected plane by using an excitation that is accomplished by means of a particular electrode combination.

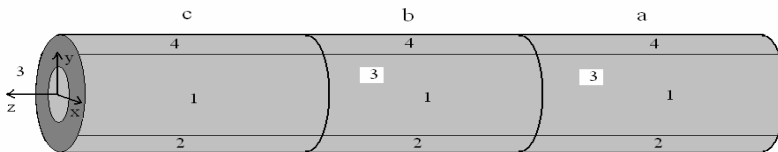


Fig. 1. Scheme of the piezoelectric actuator with the sectioned electrode

Sections *a* and *c* have equal length, meanwhile length of section *b* is selected so as it would coincide with the length of half-wave of the 3<sup>rd</sup> flexural vibration mode between two oscillation nodes, i.e. from 0,356 to 0,644 with respect to cylinder length *L*. The width of each electrode is equal to 1/4 of perimeter of the outer circle of the cylinder. The electrodes are oriented so that their centers coincide with the intersections of the cylinder surface and coordinate planes *xOz* and *yOz*. The purpose of zones *a* and *c* is to generate vibrations in a selected plane. Zone *b* is used for excitation of longitudinal vibrations. The following excitation schemes of electrodes are applied when it is necessary to induce vibrations in a selected particular plane:

I – vibrations in *xOz* plane are generated when  $\cos\alpha$  excitation signal is applied to electrode sections a1, a4, b2, b3, c1, c4 and  $\cos(\alpha + \phi)$  signal – to a2, a3, b1, b4, c2, c3;

II – vibrations in *yOz* plane are generated when  $\cos\alpha$  excitation signal is applied to electrode sections a1, a2, b3, b4, c1, c2 and  $\cos(\alpha + \phi)$  signal – to a3, a4, b1, b2, c3, c4;

III - vibrations in *xyz* space are generated when  $\cos\alpha$  excitation signal is applied to electrode sections a1, b1, b2, b3, b4, c1,  $\cos(\alpha + \pi/2)$  signal – to a2, c2,  $\cos(\alpha + \pi)$  signal – to a3, c3 and  $\cos(\alpha + 3\pi/2)$  signal – to a4, c4.

During excitation phase difference  $\phi$  is selected in the range of  $-\pi \div \pi$  by considering the shape of contact point trajectory required for generation. The central electrode is grounded.

The prototype of the piezoelectric actuator was fabricated from PI transducer PT130.00, which is manufactured from piezoceramic material of type PIC151. Dimensions of the piezoactuator are  $D = 3,2$  mm,  $d = 2,2$  mm,  $L = 24$  mm. It is excited by applying voltage of 10 V with phase difference of  $\phi = \pi/2$ .

## 2. Results of finite element modeling

Finite element (FE) model of the piezoelectric actuator (Fig. 2) was built by means of software ANSYS v.11. Finite element SOLID5 was used for meshing of the actuator structure, which was assumed to be monolithic and characterized by ideal polarization. The actuator is modeled as not clamped. The electrodes were formed by grouping nodes of the elements and assigning voltage 10 V or 0 V (in the case of grounding).

Numerical analysis of the piezoelectric actuator started from modal analysis with the purpose to obtain the required structural configuration of the piezoactuator, i.e. to determine a particular ratio of piezoactuator length *L* and diameter *D* as well as to define electrode topology that allows to achieve the 3<sup>rd</sup> flexural mode and the 1<sup>st</sup> longitudinal mode at the same resonant

frequency. The first task was determination of the required electrode topology since it influences the stiffness of the whole system.

The piezoelectric actuator has to generate vibrations not only in one plane but also in a plane that is perpendicular to the former, i.e.  $xOz$  and  $yOz$ . Therefore the perimeter of the modeled structure was divided into 4 sections and its length – into 3 sections: the first – from 0 to 0,356, the second – from 0,356 to 0,644 and the third – from 0,644 to 1 with respect to the cylinder length  $L$ .

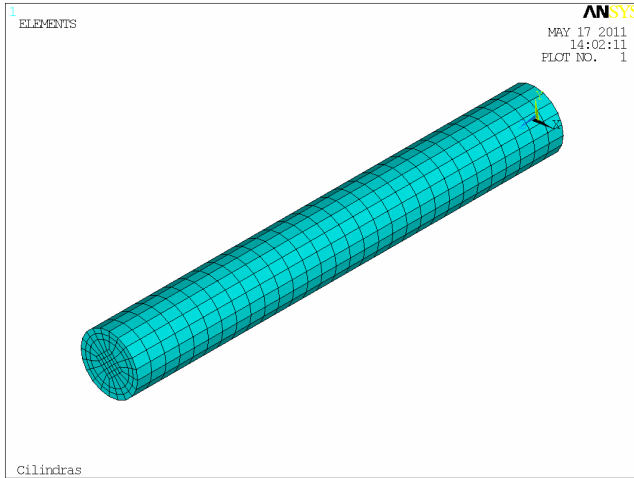


**Fig. 2.** Finite element model of the developed piezoelectric actuator

Lists of the vibration modes and the corresponding resonant frequencies obtained from finite element simulations for the piezoelectric actuator are provided in Table 1. The modeled structure is symmetrical therefore the resonant frequencies coincide in the case of modes located in different planes.

**Table 1.** Vibration modes and the corresponding resonant frequencies of the actuator

Vibration mode	Resonant frequency, Hz
I flexural	13793
II flexural	35889
III flexural	65250
I longitudinal	65639

In the subsequent stage of simulations the piezoactuator was subjected to harmonic analysis, which was performed by sweeping through frequencies from 60 to 80 kHz with a 50 Hz step. Numerical results are presented in Fig. 3, which illustrates dependencies of the length of the major and minor semi-axes of elliptical trajectories as the function of excitation frequency. The peaks in the curves correspond to particular resonance of the actuator i.e. the first peak corresponds to the 1<sup>st</sup> flexural mode, while the last peaks correspond to the 1<sup>st</sup> longitudinal and 3<sup>rd</sup> flexural modes.

Only the 3<sup>rd</sup> flexural and the adjacent 1<sup>st</sup> longitudinal modes will be considered. Fig. 4 illustrates motion trajectories obtained from the simulations for the case when the piezoactuator vibrates in its 3<sup>rd</sup> flexural mode by applying the aforementioned schemes I and II. These results indicate that during excitation with the scheme I the trajectory of the contact point has major semi-axis that is parallel to the  $x$  axis. Excitation with the scheme II results in a motion trajectory with the major semi-axis being parallel to the  $y$  axis.

During excitation with the scheme III the spatial trajectory is obtained that is suitable for generation of the rotational motion of a rotor (Fig. 4c). Top of the ellipse is located at a distance that is sufficiently large in order to induce a torque capable of moving a rotor.

The provided simulation results also demonstrate the amplitude variations for the longitudinal vibrations, which depend on quantity of excited electrodes. Larger excited area of the piezoactuator leads to a higher input energy, which, as a consequence, results in more intensive oscillations.

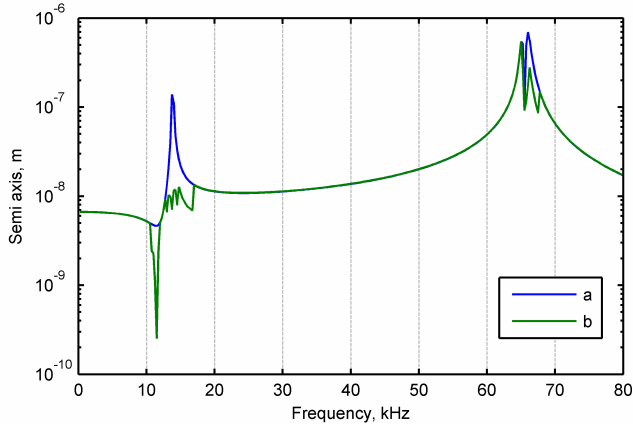


**Fig. 3.** Dependences of major and minor semi-axes of elliptical trajectories as a function of frequency

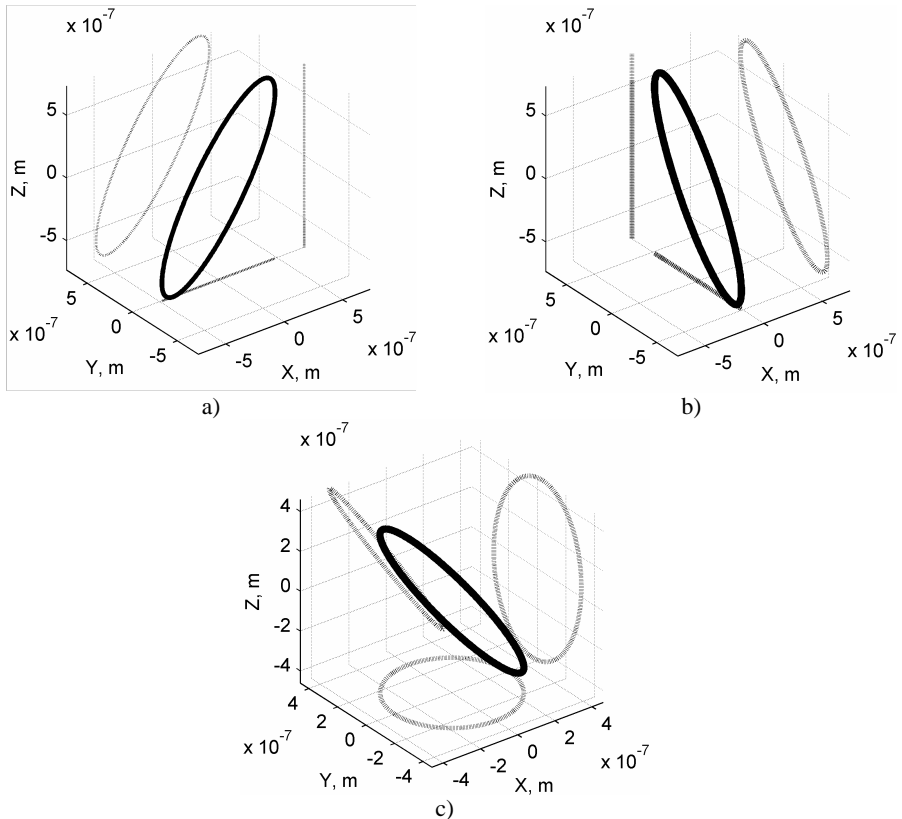


**Fig. 4.** Simulated trajectories of the actuator contact point under different excitation schemes:  
 a) 1<sup>st</sup> excitation scheme, b) 2<sup>nd</sup> excitation scheme, c) 3<sup>rd</sup> excitation scheme

## 2. Experimental results

The prototype actuator was built (Fig. 5c). The electrodes were formed from silver by means of the electric arc and a special high precision machine.

The procedure of electrode formation was carried out locally and did not alter temperature of the piezoceramic material across its volume. Therefore it was assumed that the formation of the electrodes had no influence on the quality of the polarization.

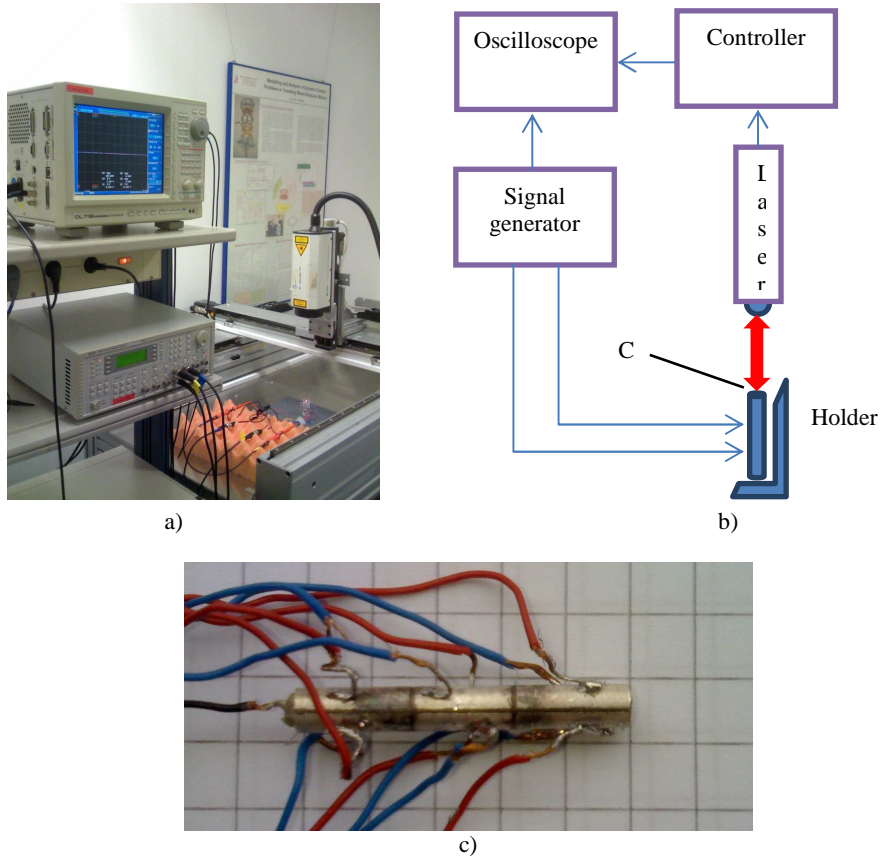


**Fig. 5.** Scheme of a setup used for laser measurements of vibrations (a, b); experimental prototype of the actuator with radial polarization (c); (CP – contact point)

Fig. 5b provides a setup of laboratory equipment that was used for the testing of the developed actuator. The device was positioned in the holder of the foam rubber that was placed on the table. Thereby it is assumed that a soft and non-viscous layer of the foam will not damp down the resonant frequencies of the actuator (i.e. it is assumed that in this way the piezoactuator is in a free position). The piezoactuator was driven by the 4-channel generator Wavetek 195 through a voltage amplifier EMI 1040L by employing the aforementioned electrode excitation schemes. The output from the amplifier was also fed to the oscilloscope Yokogawa DL716 in order to be able to determine the phase difference between driving signal and the measured one. Vibrations of the contact point of the piezoactuator were registered by means of laser Doppler vibrometer Polytec CLV-3D. The measured signal was processed by vibrometer controller Polytec CLV-3000, which after decoding provides voltage output

proportional to vibrational velocity components  $v_x$ ,  $v_y$  and  $v_z$ . The registered signal is subsequently transferred to the oscilloscope for recording and further processing.

The described experimental setup was used to measure resonant frequencies of the fabricated piezoactuator. Results of the measurements are listed in Table 2. Comparison of simulated resonant frequencies in Table 1 with the respective experimental findings reveals that the latter are slightly shifted towards lower frequencies. However, the experimental and numerical values of resonant frequencies are in a close agreement since the largest difference between results does not exceed 7 %. Thus it is possible to state with confidence that the developed finite element model confirms to the physical one.

**Table 2.** Measured resonant frequencies of the radially-polarized piezoactuator

Vibration mode	Resonant frequency, Hz
I flexural	13000
II flexural	34000
III flexural	60040
I longitudinal	64380

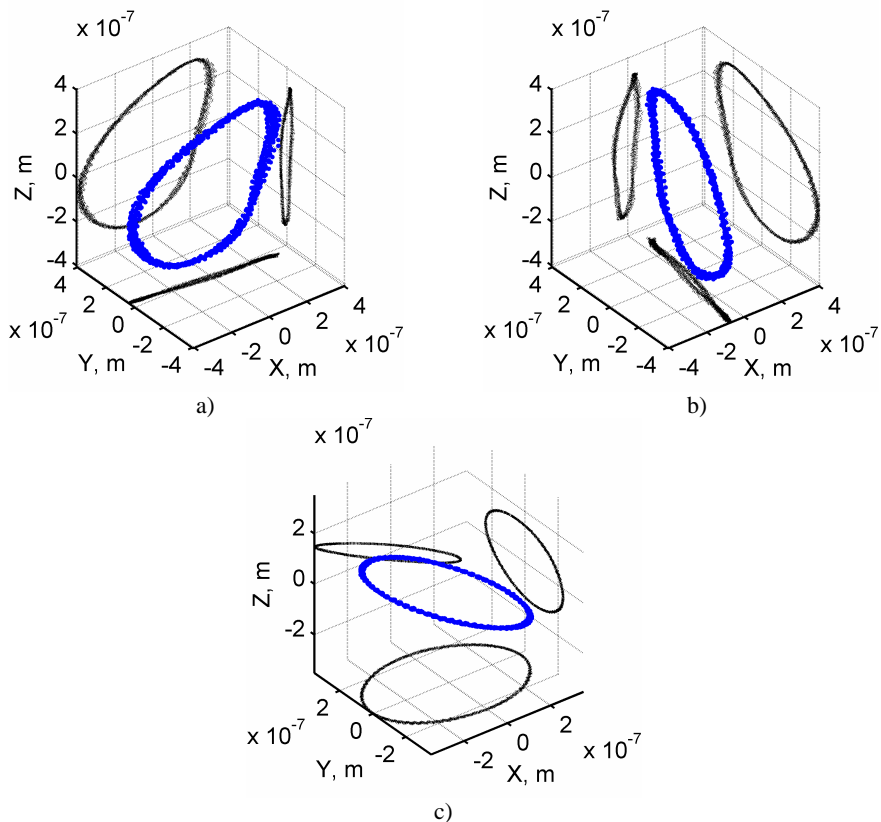


**Fig. 6.** Measured trajectories of the actuator contact point under different excitation schemes: a) 1<sup>st</sup> excitation scheme, b) 2<sup>nd</sup> excitation scheme, c) 3<sup>rd</sup> excitation scheme

The experimental setup was also used to measure trajectories of the contact point motion. The excitation regimes (schemes and excitation voltage amplitudes) used for the measurements fully correspond to those applied during the simulations. The vibrometer measured velocity components  $v_x$ ,  $v_y$  and  $v_z$ , that, after decoding, were proportional to the voltage output of the

controller. Velocity range of 25 mm/s/V was used. The results allowed to determine the coordinates of each trajectory point. Fig. 6 illustrates the measured contact point trajectories obtained when the piezoactuator was excited by applying earlier described excitation schemes.

**Table 3.** Numerically and experimentally obtained parameter of the ellipses

Parameters	Numerical results			Experimental results		
	No.1	No.2	No.3	No.1	No.2	No.3
Length of major semi-axis, $\mu\text{m}$	0.518	0.517	0.511	0.395	0.397	0.392
Length of minor semi-axis, $\mu\text{m}$	0.262	0.263	0.509	0.256	0.255	0.354
Axis angle in xy plane	0°	90°	176°	-6°	10°	168°
Axis angle in xz plane	58°	90°	125°	28°	28°	158°
Axis angle in yz plane	90°	56°	103°	83°	78°	86°

Measurement results reveal that the experimental elliptical trajectories of the contact point are located in one plane, which again confirms the accuracy of the FE model. Detailed comparison between numerical and experimental results is given in Table 3.

## Conclusions

Numerical and experimental investigation of the piezoelectric actuator with radial polarization confirms that elliptical trajectory of contact point motion can be achieved in three directions independently. Three separate directions of contact point elliptical motion were obtained during numerical simulations and confirmed by experimental study. It demonstrates that a 3-DOF motion of the slider can be achieved. Results of the simulations and experimental measurements are in a good agreement and confirm the ability of the developed FE model of the piezoelectric actuator to provide sufficiently reliable numerical results.

## Acknowledgment

This work has been supported by the Research Council of Lithuania, project No. MIP-122/2010. This research was also performed under EU Structural Funds project "Postdoctoral Fellowship Implementation in Lithuania". The authors would like to sincerely thank dr. Tobias Hensel and his team for the assistance in making experimental research that was performed at Paderborn University in the laboratories of the Mechatronics and Dynamics Department.

## References

- [1] **Uchino K.** Piezoelectric Actuators and Ultrasonic Motors. Kluwer Academic Publishers, Boston, 1997, 364 p.
- [2] **Uchino K., Giniewicz J.** Micromechatronics, Marcel Dekker Inc., New York, 2003.
- [3] **Bansevičius R., Ragulskis K.** Vibromotors. Vilnius, 1981. p. 289 (in Russian).
- [4] **Ragulskis K., Bansevičius R., Barauskas R., Kulvietis G.** Vibromotors for Precision Microrobots. New York: Hemisphere Publishing, 1988, 325 p.
- [5] **Bansevičius R., Kulvietis G., Mažeika D.** Numerical Identification of Modal Shapes Sequence of Multicomponent Piezoelectric Actuators, Journal of Vibroengineering, Vol. 4, 2000.
- [6] **Calas H., Moreno E., Eiras J., Aulet A., Figueredo J., Leija L.** Non-uniformly polarized piezoelectric modal transducer: fabrication method and experimental results, Smart Materials and structures, Vol.15(4), pp. 904-908, 2006.
- [7] **Lučinskis R., Mažeika D., Hensel T., Bansevičius R.** The experimental research of piezoelectric actuator with two vectors of polarization direction. – Mechanika. –Kaunas: Technologija, 2010, No2 (82), p. 50-58.